JOURNAL OF GEOPHYSICAL RESEARCH, VOL. 100, NO. B10, PAGES 20,359–20,365, OCTOBER 10, 1995

Localized boundary layer below the mid-Pacific velocity anomaly identified from a *PcP* precursor

Jim Mori
U.S. Geological Survey, Pasadena, California

Donald V. Helmberger
Seismological Laboratory, California Institute of Technology, Pasadena

Abstract. Dense record sections from deep earthquakes in Fiji and Argentina recorded on hundreds of short-period stations in California at distances of 81° to 85° are used to investigate the detailed *P* wave velocity structure above the core-mantle boundary (CMB). In the Fiji data a secondary phase arriving 2 to 4 s after the direct *P* is identified as a precursor to *PcP*. This phase provides good evidence for a reflection off the top of a thin low-velocity layer above the CMB. Comparisons to synthetic seismograms indicate a layer thickness of 10 km and a velocity reduction of 5%–10% compared to the overlying mantle. A record section from an Argentina event does not show the *PcP* precursor, indicating that the low-velocity layer is not a global feature. This thin low-velocity layer is in the same place as a much larger *S* wave velocity anomaly in the lower mantle and is probably indicative of a boundary layer just above the CMB under the mid-Pacific.

Introduction

Detailed information about the compressional (*P* wave) velocity at the base of the mantle above the core-mantle boundary (CMB) provides important constraints on the mechanisms of heat transfer that help drive the convection in the mantle [*Loper and Lay*, 1995]. Part of the heat for driving the convection is thought to come from a thermal boundary layer at the base of the mantle, and there has been much interest in searching for sharp velocity contrasts that may provide a measure of thermal and chemical changes within this layer [i.e., *Jeanloz and Richter*, 1979]. Some studies have reported zones at the base of the mantle with low *P* wave velocities [i.e., *Cleary*, 1974; *Doornbos*, 1983] and others with high *P* wave velocities [i.e., *Wright et al.*, 1985; *Vidale and Benz*, 1993]. However, most previous studies have not had the resolution to identify features on the scale of a few tens of kilometers or less that is necessary to identify boundary layers. One recent investigation by *Vidale and Benz* [1992] that could identify smaller-scale features reported a simple CMB with no unusual velocity contrasts under the northeast Pacific.

In this study we use dense record section to provide high-resolution information about the *P* wave velocity structure above the CMB. Data generated from two deep earthquakes in Fiji recorded in California show a secondary *P* arrival that is most likely a reflection from a strong velocity contrast above the CMB. In contrast to the Fiji data a similar record section from an Argentina earthquake does not have any indication of a low-velocity layer. The existence of this low-velocity layer may be correlated with larger-scale velocity anomalies that are observed in the lower mantle and thus may have an important role in the thermal structures that control mantle convection.

Paper number 95JB02243.
0148-0227/95/95JB-02243$05.00

Data

This study takes advantage of the hundreds of short-period stations operated in California by the U.S. Geological Survey (USGS) and California Institute of Technology in Pasadena. Stations are spread out over an area roughly 1100 × 250 km with spacings of 15 to 30 km (Figure 1). There can be large differences in the waveforms of adjacent stations, and this incoherence at short periods has often hampered high resolution studies of the Earth's interior. Much of the large site-to-site variation is attributed to near-surface structure [i.e., *Mori and Frankel*, 1992] and can vary over distances smaller than the station spacing. One method to overcome the problem is to combine recordings from hundreds of stations and look for features of the waveforms that are correlated over many stations [*Benz et al.*, 1994]. For noise due to uncorrelated site response the signal to noise ratio should increase as the square root of the number of stations. In this study we used a large number of teleseimic waveforms to look for *P* wave interactions near the CMB in data from deep earthquakes in Fiji and Argentina (Table 1). Using stacked record sections, we are able to resolve a secondary phase that arrives a few seconds after the direct *P*. In addition to stacking traces from a single event, we were able to combine two closely spaced Fiji events into the same record section to further densify the data.

Figure 2 shows an example of the data and processing used to resolve the details of the teleseismic *P* waves. The left panel contains a subset of the displacement data waveforms for the Fiji record section in the limited distance range of 82° to 83°, showing the spatial density of the data. To obtain the displacement waveforms, the original data were band-pass filtered between 0.2 and 10 hz and corrected for the short-period instrument response [*Stewart and O'Neill*, 1980]. The seismograms were lined up to a common start time by using the lag time that corresponded to the maximum cross correlation between the trace and an averaged version of all the traces. A small secondary phase about 2 s after the direct *P* wave can be seen in many of the traces, but it is difficult to clearly see its amplitude

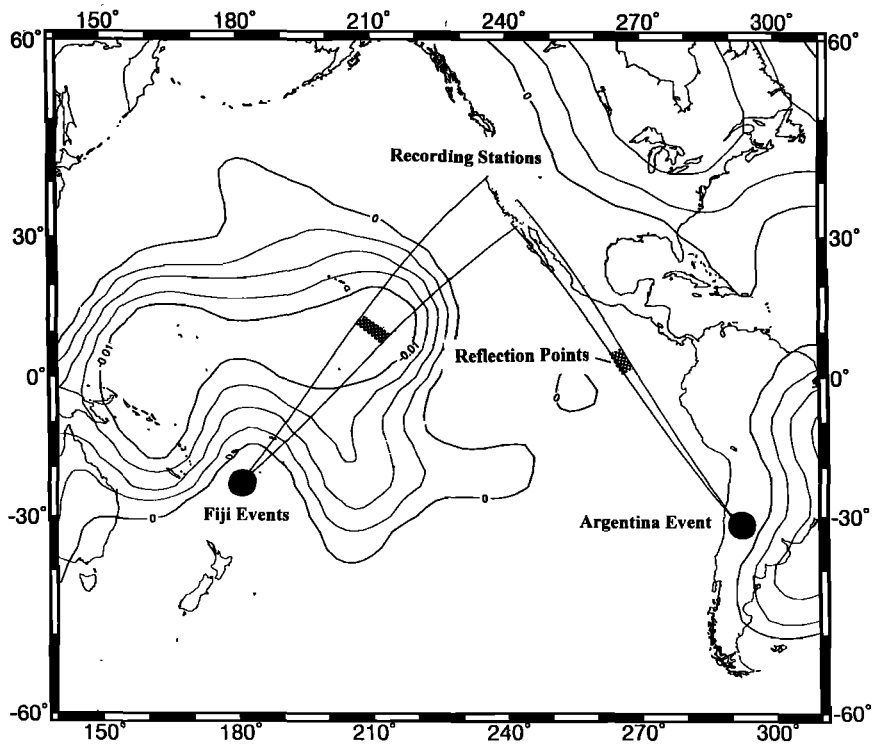

Figure 1. Locations of earthquakes (solid circles) used in this study and the great circle paths to the recording stations in California (light stippled area). Dark stippled areas show where the waves bottom close to the core-mantle boundary (CMB). Contours show *S* wave velocities in the lowest portion of the mantle (2890 km depth) from *Su et al.* [1994]. Contour units are multiplicative factors from the average velocity.

and polarity. The displacement data were stacked within 20 km bins, with each bin containing 5 to 40 traces. The middle panel of Figure 2 shows the stacked traces plotted at 20 km intervals. The same process was used on the velocity waveforms, and the resultant velocity stack is shown in the right panel of Figure 2. We display both the displacement and velocity data since it is easier to identify the polarity of secondary arrivals on the displacement records, while the velocity data are better for resolving the finer details in the waveforms.

The complete record sections of stacked velocity traces for the Fiji and Argentina data are shown in Figures 3 and 4, respectively. The Fiji data contain 532 traces and Argentina data contain 397 traces. The stacked Argentina data have a lower signal to noise ratio because the record section contains only one event and thus has a lower station density. Also, the *P* waves from Argentina arrive closer to the long axis of the station distribution in California, which contributes to the lower station density in the stacked record section. Compared to the Fiji data, the stacked traces of the Argentina record section have about half the number of stations. Assuming that variations in the waveforms are mainly due to uncorrelated site response effects, the noise level in the stacked Argentina data would be $\sqrt{2}$ times higher than in the Fiji record section, which is consistent with the observed data.

Precursor to *PcP*

The waveforms from the Fiji record sections in Figures 2 and 3 clearly show a secondary arrival that is 2 to 4 s after the direct *P*. The secondary arrival has a different apparent velocity that is about 15% faster than the direct *P*. Since we have lined up the data on the first arrival, we have lost information about the absolute timing, but if we assume that the direct *P* has an apparent velocity of 21.6 to 22.2 km/s [*Kennett*, 1991], then the secondary arrival has an apparent velocity of 24.7 to 25.6 km/s. The different apparent velocity relative to the direct *P* indicates that the phase is not due to near-source nor near-receiver structure. An important observation is that this phase appears to have the opposite polarity from the *P*, which is seen most clearly in the displacement waveforms of Figure 2. The opposite polarity relative to the direct *P* implies that the arrival is not *PcP*. Reasonable velocity structures of the CMB produce *PcP* phases with the same polarity as the direct *P*. Also, the *P* and *PcP* takeoff angles are not close to nodal planes, so the

Table 1. Location and Magnitudes of Earthquakes Used in This Study

	Date	Time, UT	Latitude	Longitude	Depth, km	m_b
Fiji	Sept. 17, 1982	1328:24.8	23.407°S	179.852°W	546	5.9
Fiji	Oct. 10, 1990	0554:53.5	23.497°S	179.029°W	549	6.0
Argentina	Oct. 10, 1993	1759:02.7	31.704°S	68.232°W	107	5.9

Taken from monthly bulletins of the National Earthquake Information Center.

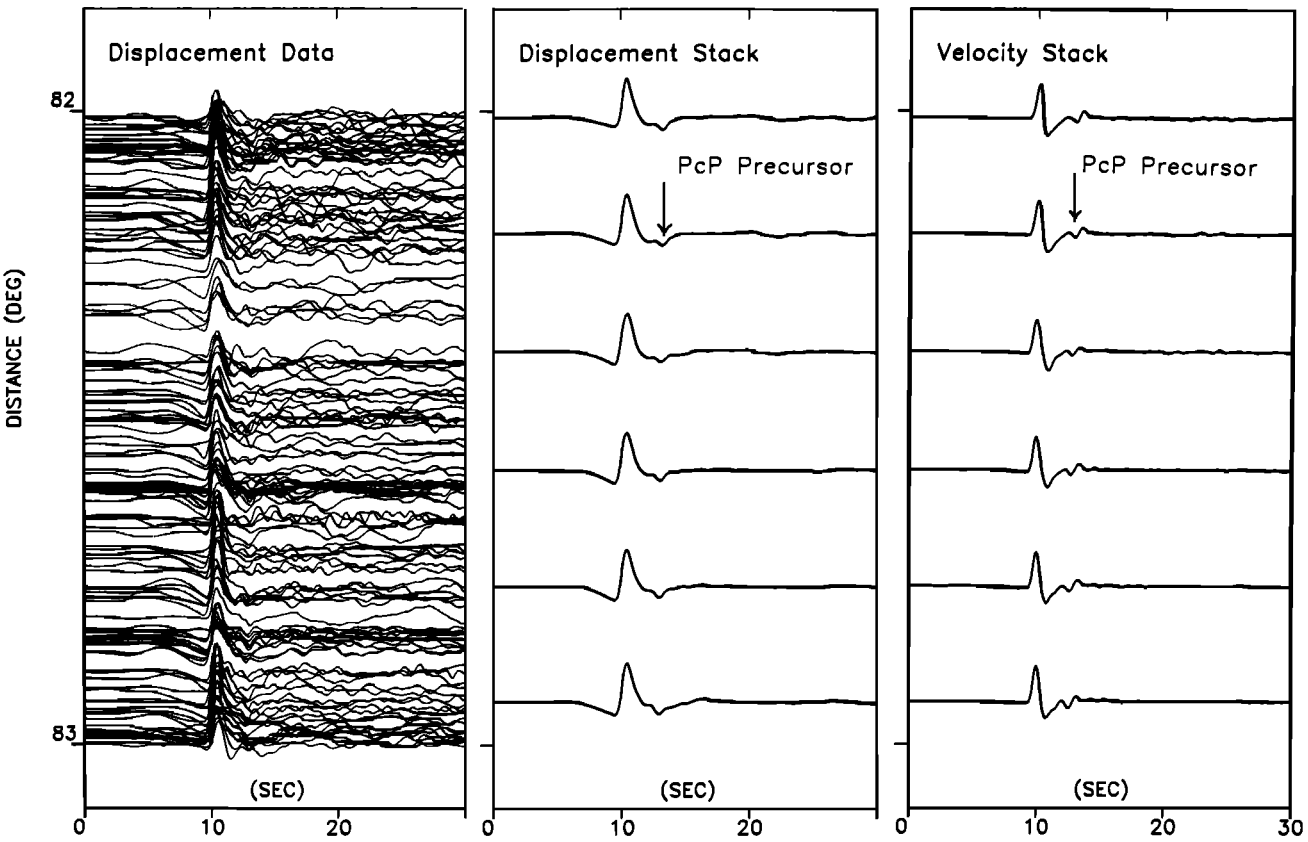

Figure 2. Detail of the Fiji record section showing the density of data and the results of the signal processing. The left panel shows the displacement waveforms used to construct the record section. Middle panel shows the displacement data stacked by averaging over traces were within 20 km distances. Right panel shows the results of the same stacking procedure for velocity data.

difference in polarity cannot be attributed to the focal mechanism. There is little evidence for sharp velocity contrasts below the CMB in the liquid core [*Stevenson*, 1987; *Garnero et al.*, 1993], so any fine velocity structure in the region of the CMB is most likely above the discontinuity. From the reversed polarity and the timing relative to the direct *P* we conclude that the secondary arrival is a reflection from a low-velocity layer above the CMB, and thus it is a phase that would arrive earlier than *PcP*.

In contrast to the Fiji record section the data from Argentina show no significant phases in the 15-s time window following the direct *P*. The lack of observable secondary phases from Argentina implies that there are no large velocity contrasts above the CMB in the region under western Mexico where these rays bottom. Another possibility is that there can be strong velocity contrasts in this region but with large amounts of spatial variability, so that there are no coherent arrivals in the stacked data of Figure 4. However, in this case, one might expect to see secondary phases in limited distance ranges of the record section, and there are no indications of such arrivals.

Comparison to Synthetics

We generated synthetic seismograms to model the Fiji record section using a generalized ray code with simple one-dimensional structures. This program has been tested against reflectivity methods in previous studies [*Lay and Helmberger*, 1983]. We did not attempt to model the earthquake source directly but used an empirical source function approach [*Gilbert and Helmberger*, 1972]. The source time function was created by averaging together 2.5 s of the direct *P* wave from all the data.

Synthetics were calculated for a suite of velocity models that had low-velocity layers above the CMB with varying thicknesses and velocity contrasts. Changes in the *S* wave velocity contrast and density had virtually no affect on the waveforms. The relative phase, timing, and amplitude of the *PcP* precursor, compared to the direct *P*, provide strong constraints on the *P* wave velocity contrast at the top of the low-velocity layer and weaker constraints on its thickness. The relatively large backswing on the *PcP* precursor, as seen in the velocity data of Figure 3, indicates interference with *PcP* and helps constrain the thickness of the low-velocity layer and the *P* wave velocity contrast at the CMB. Figure 3 shows synthetic seismograms for a model that provides a good fit to the data. This preferred model has a 10-km-thick layer above the CMB with a *P* wave velocity drop of 5% from the lower mantle. This structure is the Preliminary Earth Model (PREM) by *Dziewonski and Anderson* [1981] with a 5% velocity reduction at the base of the mantle.

It is difficult to establish a unique model given only the short-period reflected phase, but one can gain some appreciation of the constraints by performing sensitivity tests. Five

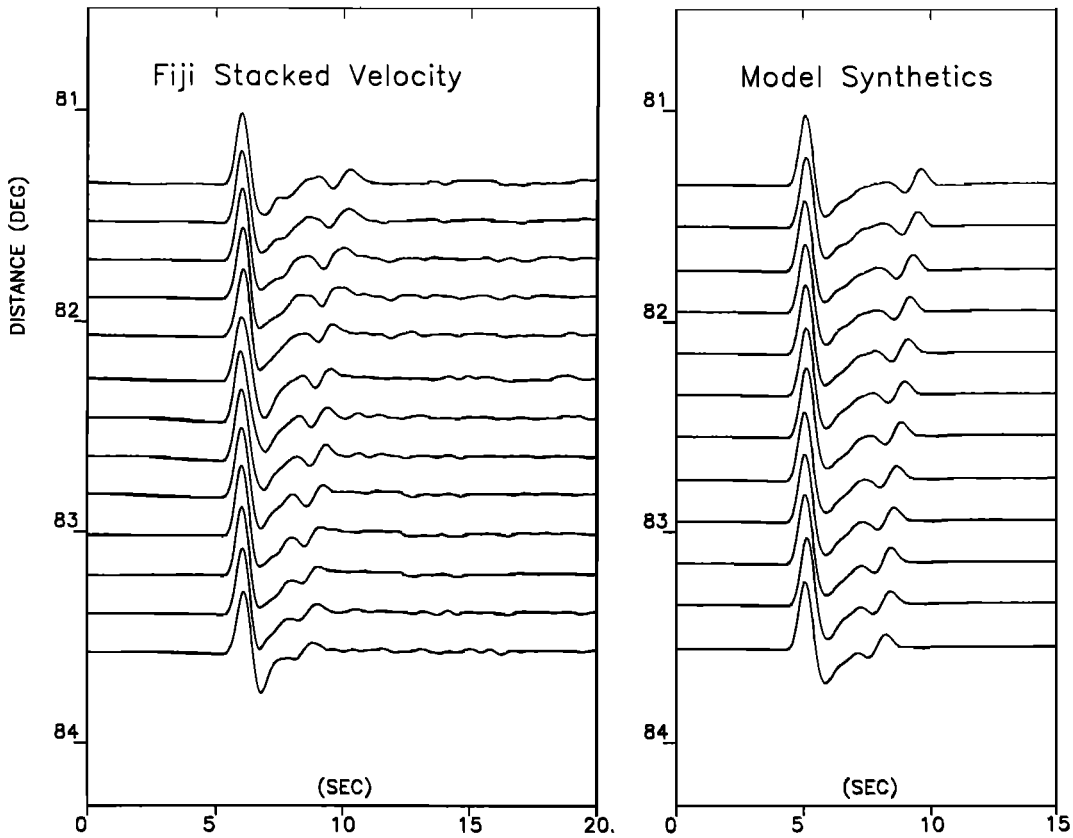

Figure 3. Stacked velocity data for (left) the two Fiji events and (right) synthetics calculated for a the preferred model of a 10-km layer above the CMB. There is a 5% velocity contrast with the overlying mantle.

examples that vary some of the parameters are presented in Figure 5: Figure 5a is the same model as in Figure 4, except the layer velocity was reduced by 10%, instead of 5%; Figure 5b is the same as Figure 5a, except the *PcP* phase is not included; Figure 5c is the same as Figure 5a, except synthetics were stacked using the same procedures used for the observed data; Figure 5d is the preferred model used in Figure 4; and Figure 5e is PREM.

The shape of the secondary arrivals in synthetics in Figures 5a, 5c, and 5d are strongly controlled by the relative timing between the *PcP* precursor and *PcP* thus providing a good constraint on the thickness of the low-velocity layer. From comparisons with the data we estimated the layer thickness to be 10 km. From the relative amplitudes between the direct *P* and the secondary arrival we estimated a 5% velocity contrast.

An alternate interpretation of the data is that the secondary phase is only because of the reflection off the top of the low-velocity layer with no contributions from *PcP*. For this interpretation the synthetic in Figure 5b shows the true size of the reflection coefficient from the top of a low-velocity layer with a 10% contrast, without any *PcP* interference. There are plausible reasons why *PcP* could have negligible amplitudes in our data, such as scattering from small perturbations in the core-mantle impedance. In this case, matching the relative amplitudes of the synthetics to the data indicates a larger velocity contrast of 10% for the low-velocity layer, with no constraint on its thickness.

Because the shape of the secondary arrival has a large backswing, we prefer the interpretation that includes a contribution from *PcP*. In Figure 6 the *PcP* precursor (labeled P_r) is the downward arrival about 3 s after the direct *P*. *PcP* is the upward arrival about 1 s after the precursor. This interpretation enables us to estimate both the layer thickness and velocity contrast and results in our preferred model of a 10-km-thick low-velocity layer with a 5% contrast. The resolution of our estimate of the layer thickness is demonstrated in Figure 6, where we show synthetics for layer thicknesses of 5, 10, 15, and 20 km using a velocity contrast of 5%. For a 5-km layer the *PcP* arrives soon after the *PcP* precursor and the two phases destructively interfere, producing a secondary arrival that is too small compared to the data. For the 15- and 20-km-thick layers the timing between the *PcP* precursor (down of the secondary arrival) and *PcP* (up in the secondary arrival) is spread out too much compared to the data. The 10-km layer provides the best fit to the data. As an alternative to a single low-velocity layer, the effect of a negative gradient, was tested by including two layers with 2.5% and 5% velocity drops within the 10-km thickness. The bottom trace of Figure 6 shows that this case has a *PcP* precursor that is too small compared to the data. From these calculations we conclude that the layer thickness is greater than 5 km and less than 20 km with the best fit at 10 km. Also, a negative velocity gradient, in place of a single layer, does not fit the data very well.

All of the modeling and conclusions about the velocities are based on one-dimensional structures. It is likely that the secondary arrival can also be modeled with more complicated two- and three-dimensional structures [i.e., *Kampfmann and Muller*, 1989] that may have less, or possibly no, low-velocity

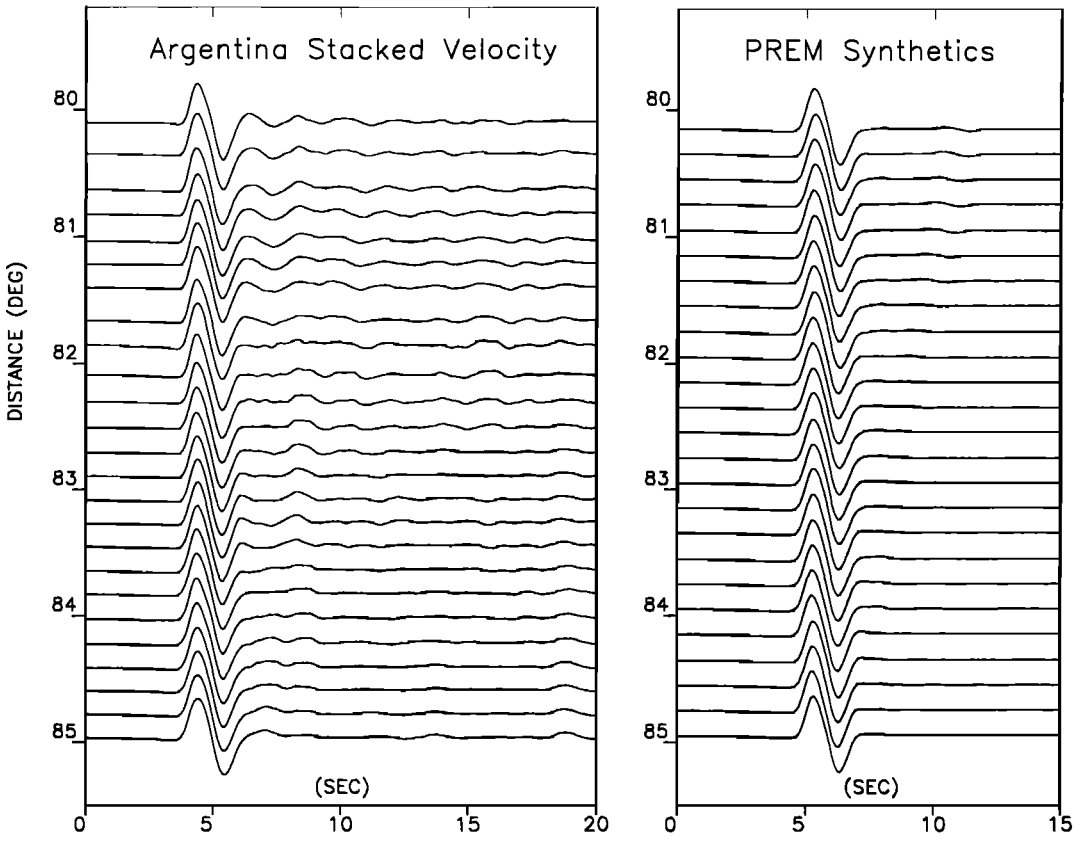

Figure 4. Stacked velocity data for (left) the Argentina event and (right) synthetics calculated for the Preliminary Earth Model (PREM) which has no fine structure above the CMB.

contrast at the base of the mantle. In this study, we use a simple one-dimensional structure that can easily match the data. Further studies using other earthquakes need to be done to map out the lateral extent of this low-velocity feature and resolve whether or not there are strong effects from CMB topography.

Synthetic seismograms were also calculated using PREM and compared to the Argentina record section to show that these data are consistent with a velocity model that has no fine structure above the CMB (Figure 4). As in the Fiji case, the Green functions were convolved with a source time function that is an average of 2.5 s of the direct *P* wave from all the data. Without any velocity contrasts above the CMB there are essentially no secondary phases after the direct *P*. Even at the CMB the combination of velocity and density contrasts produces a small reflection coefficient, so the *PcP* amplitudes are very small in this distance range.

Discussion

The Fiji record section of this study shows a clear *PcP* precursor of reversed polarity that is inferred to be a reflection from a low-velocity zone above the CMB. From the two examples in this study we speculate that there may be a correlation between the existence of this layer and the larger-scale velocity anomalies of the lower mantle seen in various velocity models [i.e., *Su et al.*, 1994]. The path for which we observed the low-velocity layer in the Fiji data has its reflection point within the large mid-Pacific low-velocity anomaly (Figure 1). Also, we do not observe the low-velocity layer along the other path from Argentina, which does not pass near any strong velocity anomalies (Figure 1). This association of a thin low-velocity layer at the base of the mantle with the large mid-Pacific anomaly was also observed by *Garnero and Helmberger* [1995] from differential travel times between *SKS* and SP_dKS. If there is a physical basis for the correlation, one might expect there to be even larger *P* wave velocity contrasts in other localized regions above the CMB. The region of the lower mantle under the mid-Pacific examined in this study is not in the strongest part of the large *S* wave anomaly, and other regions that have even lower *S* wave velocities may have correspondingly larger *P* wave velocity contrasts.

A thin (~10 km) low-velocity zone with a strong velocity contrast (5% to 10%) is a good candidate for a boundary layer above the CMB. There is a question whether such a layer could be a temperature feature [i.e., *Jeanloz and Richter*, 1979; *Williams and Jeanloz*, 1990], a compositional contrast [i.e., *Knittle and Jeanloz*, 1989], or both [i.e., *Wysession et al.*, 1992; *Yuen et al.*, 1993]. Either higher temperatures of a thermal boundary layer or larger densities of a chemical boundary layer would produce the low velocities, so it is difficult to make this distinction from these seismic data alone. In either case the importance of the thin layer is that it underlies a large lower mantle anomaly in the mid-Pacific, which is interpreted to be indictive of mantle upwelling [*Su et al.*, 1994]. This suggests that this low-velocity feature is a boundary layer that provides a significant portion of the heat and/or density contrasts that drive mantle convection.

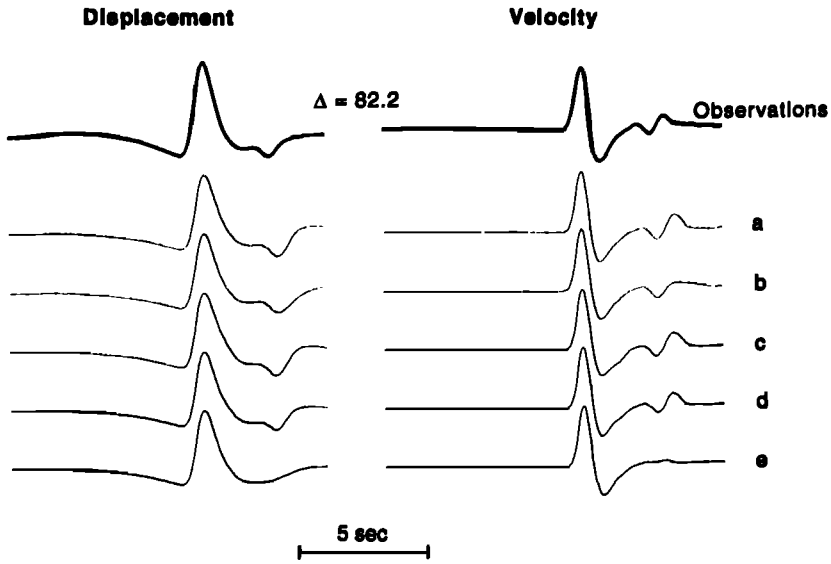

Figure 5. Sensitivity tests displaying (left) stacked displacement and (right) velocity for Fiji data at a range of 82.2°. Synthetics calculations are done for (a) PREM with 10% low-velocity layer and 10 km thickness at the base of the mantle, (b) same as Figure 5a without *PcP*, (c) numerical stack of seismograms calculated using a model in Figure 5a averaged over a 20-km-distance range, (d) same as Figure 5a except with a 5% velocity reduction, and (e) PREM.

Conclusions

We have used a dense record section of short-period seismograms from two earthquakes in Fiji to resolve a secondary arrival that has been identified as a reflection off the top of a low-velocity layer above the CMB. We estimate a layer thickness of 10 km and a strong velocity contrast of 5%–10% with the overlying mantle. Similar data from an earthquake in Argentina do not show this reflection, indicating that the low-velocity layer is a localized feature. The association of the low-velocity layer with a large-scale lower mantle velocity anomaly in the mid-Pacific suggests that it is a thermal and/or chemical boundary layer that may drive a mid-Pacific upwelling.

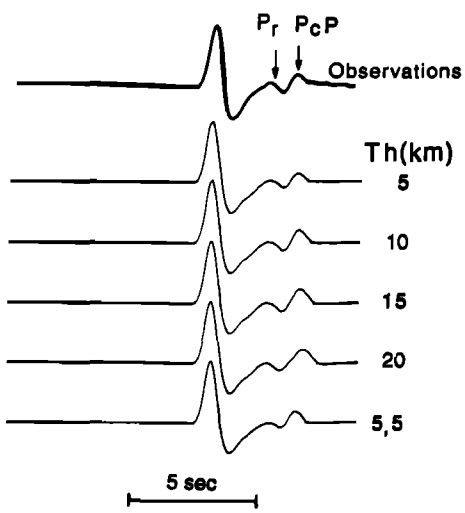

Figure 6. The estimate of the layer thickness is demonstrated by displaying (top) the stacked velocity for the Fiji data at a range of 82.2° with synthetic calculations for various thicknesses. The *PcP* precursor (P_r) and *PcP* arrivals are indicated in the observed data. The bottom trace shows the effect of simulating a negative gradient across a 10-km thickness at the base of the mantle.

Acknowledgments. Helpful comments on this paper were provided by J. Vidale, G. Choy, T. Lay, J. Revenaugh, and M. Wysession. Xiangming Ding helped with Figure 1. This research was supported in part by NSF grant EAR9316441. Contribution 5564, Division of Geological and Planetary Sciences, California Institute of Technology.

References

Benz, H. M., J. E. Vidale, and J. Mori, Using regional seismic networks to study the Earth's deep interior, *Eos Trans. AGU*, *75*(20), 225 and 229, 1994.

Cleary, J. R., The D″ region, *Phys. Earth Planet. Inter.*, *30*, 13–27, 1974.

Doornbos, D. J., Present seismic evidence for a boundary-layer at the base of the mantle, *J. Geophys. Res.*, *88*, 3498–3505, 1983.

Dziewonski, A. M., and D. L. Anderson, Preliminary reference Earth model, *Phys. Earth Planet. Inter.*, *25*, 297–356, 1981.

Garnero, E. J., and D. V. Helmberger, A very slow basal layer underlying the large-scale low-velocity anomalies in the lower mantle beneath the Pacific: Evidence from core phases, *Phys. Earth Planet. Inter.*, in press, 1995.

Garnero, E. J., D. V. Helmberger, and S. P. Grand, Constraining outermost core velocity with SmKS waves, *Geophys. Res. Lett.*, *20*, 2463–2466, 1993.

Gilbert, F., and D. V. Helmberger, Generalized ray theory for a layered sphere, *Geophys. J. R. Astron. Soc.*, *27*, 57–80, 1972.

Jeanloz, R., and F. M. Richter, Convection, composition, and the thermal state of the lower mantle, *J. Geophys. Res.*, *84*, 5497–5504, 1979.

Kampfmann, W., and G. Muller, *PcP* Amplitude calculations for a core-mantle boundary with topography, *Geophys. Res. Lett.*, *16*, 653–656, 1989.

Kennett, B. L. N., IASPEI 1991 seismological tables, 167 pp., Res. Sch. of Earth Sci., Aust. Natl. Univ., 1991.

Knittle, E., and R. Jeanloz, Simulating the core-mantle boundary: An experimental study of high-pressure reactions between silicates and liquid iron, *Geophys. Res. Lett.*, *16*, 609–612, 1989.

Lay, T., and D. V. Helmberger, A lower mantle *S*-wave triplication and

the shear velocity structure of D″, *Geophys. J. R. Astron. Soc.*, *75*, 799–838, 1983.

Loper, D. E., and T. Lay, The core-mantle boundary region, *J. Geophys. Res.*, *100*, 6397–6420, 1995.

Mori, J., and A. Frankel, Correlation of *P* wave amplitudes and travel time residuals for teleseisms recorded on the southern California seismic network, *J. Geophys. Res.*, *97*, 6661–6674, 1992.

Stevenson, D. J., Limits on lateral density and velocity variations in the Earth's outer core, *Geophys. J. R. Astron. Soc.*, *80*, 311–319, 1987.

Stewart, S. W., and M. E. O'Neill, Calculation of the frequency response of the USGS telemetered short-period seismic system, *U.S. Geol. Surv. Open File Rep.*, *80-143*, 83 pp., 1980.

Su, W.-J., R. L. Woodward, and A. M. Dziewonski, Degree 12 model of shear velocity heterogeneity in the mantle, *J. Geophys. Res.*, *99*, 6945–6980, 1994.

Vidale, J. E., and H. M. Benz, A sharp and simple section of the core-mantle boundary, *Nature*, *359*, 627–629, 1992.

Vidale, J. E., and H. M. Benz, Seismological mapping of fine structure near the base of the Earth's mantle, *Nature*, *361*, 529–532, 1993.

Williams, Q., and R. Jeanloz, Melting relations in the iron-sulfur system at ultra-high pressures: Implications for the thermal state of the Earth, *J. Geophys. Res.*, *95*, 19,299–19,310, 1990.

Wright, C., K. J. Muirhead, and A. E. Dixon, The *P* wave velocity structure near the base of the mantle, *J. Geophys. Res.*, *90*, 623–634, 1985.

Wysession, M. E., E. A. Okal, and C. R. Bina, The structure of the core-mantle boundary from diffracted waves, *J. Geophys. Res.*, *97*, 8749–8764, 1992.

Yuen, D. A., O. Cadek, A. Chopelas, and C. Matayska, Geophysical inferences of the thermal-chemical structures in the lower mantle, *Geophys. Res. Lett.*, *20*, 899–902, 1993.

D. V. Helmberger, Seismological Laboratory 252-21, California Institute of Technology, Pasadena, CA 91125. (e-mail: helm@seismo.gps.caltech.edu)

J. Mori, U.S. Geological Survey, 525 South Wilson Avenue, Pasadena, CA 91106. (e-mail: mori@bombay.gps.caltech.edu)

(Received May 8, 1995; revised July 18, 1995;
accepted July 25, 1995.)